Bounds on Lorentz Invariance Violation from Muon Fluctuations at the Pierre Auger Observatory

A. Abdul Halim,[13] P. Abreu,[67] M. Aglietta,[50,49] I. Allekotte,[1] K. Almeida Cheminant,[75,74] R. Aloisio,[42,43] J. Alvarez-Muñiz,[73] A. Ambrosone,[42] J. Ammerman Yebra,[73] L. Anchordoqui,[79] B. Andrada,[7] L. Andrade Dourado,[42,43] L. Apollonio,[55,46] C. Aramo,[47] E. Arnone,[59,49] J. C. Arteaga Velázquez,[63] P. Assis,[67] G. Avila,[11] E. Avocone,[53,43] A. Bakalova,[29] Y. Balibrea,[11] A. Baluta,[70] F. Barbato,[42,43] A. Bartz Mocellin,[78] J. P. Behler,[10] C. Berat,[*] M. E. Bertaina,[59,49] M. Bianciotto,[59,49] P. L. Biermann,[†] V. Binet,[5] K. Bismark,[35,7] T. Bister,[74,75] J. Biteau,[33,84] J. Blazek,[29] J. Blümer,[37] M. Boháčová,[29] D. Boncioli,[53,43] C. Bonifazi,[16,8] N. Borodai,[65] J. Brack,[‡] P. G. Brichetto Orquera,[7,37] A. Bueno,[72] S. Buitink,[15] M. Büsken,[35,7] A. Bwembya,[74,75] K. S. Caballero-Mora,[62] S. Cabana-Freire,[73] L. Caccianiga,[55,46] J. Caraça-Valente,[78] R. Caruso,[54,44] A. Castellina,[50,49] F. Catalani,[18] G. Cataldi,[45] L. Cazon,[73] M. Cerda,[10] B. Čermáková,[37] A. Cermenati,[42,43] K. Cerny,[30] J. A. Chinellato,[21] J. Chudoba,[29] L. Chytka,[30] R. W. Clay,[13] A. C. Cobos Cerutti,[6] R. Colalillo,[56,47] R. Conceição,[67] G. Consolati,[46,51] M. Conte,[52,45] F. Convenga,[42,43] D. Correia dos Santos,[25] P. J. Costa,[67] C. E. Covault,[77] M. Cristinziani,[41] C. S. Cruz Sanchez,[3] S. Dasso,[4,2] K. Daumiller,[37] B. R. Dawson,[13] R. M. de Almeida,[25] E.-T. de Boone,[41] B. de Errico,[25] J. de Jesús,[73] S. J. de Jong,[74,75] J. R. T. de Mello Neto,[25] I. De Mitri,[42,43] D. de Oliveira Franco,[40] F. de Palma,[52,45] V. de Souza,[19] E. De Vito,[52,45] A. Del Popolo,[54,44] O. Deligny,[31] N. Denner,[29] K. Denner Syrokvas,[28] L. Deval,[49] A. di Matteo,[49] C. Dobrigkeit,[21] J. C. D'Olivo,[64] L. M. Domingues Mendes,[16,67] Y. Dominguez Ballesteros,[27] Q. Dorosti,[41] R. C. dos Anjos,[24] J. Ebr,[29] F. Ellwanger,[37] R. Engel,[35,37] I. Epicoco,[52,45] M. Erdmann,[38] A. Etchegoyen,[7,12] C. Evoli,[42,43] H. Falcke,[74,76,75] G. Farrar,[81] A. C. Fauth,[21] T. Fehler,[41] F. Feldbusch,[36] A. Fernandes,[67] M. Fernández Alonso,[14] B. Fick,[80] J. M. Figueira,[7] P. Filip,[35,7] A. Filipčič,[71,70] T. Fitoussi,[37] B. Flaggs,[83] A. Franco,[45] M. Freitas,[67] T. Fujii,[82,§§] A. Fuster,[7,12] C. Galea,[74] B. García,[6] C. Gaudu,[34] P. L. Ghia,[31] U. Giaccari,[45] M. Giammarco,[53,43] C. Glaser,[39] F. Gobbi,[10] F. Gollan,[7] G. Golup,[1] P. F. Gómez Vitale,[11] J. P. Gongora,[11] J. M. González,[1] N. González,[7] D. Góra,[65] A. Gorgi,[50,49] M. Gottowik,[37] F. Guarino,[56,47] G. P. Guedes,[22] Y. C. Guerra,[10] L. Gülzow,[37] S. Hahn,[35] P. Hamal,[29] M. R. Hampel,[7] P. Hansen,[3] V. M. Harvey,[13] A. Haungs,[37] M. Havelka,[29] T. Hebbeker,[38] C. Hojvat,[§] J. R. Hörandel,[74,75] P. Horvath,[30] M. Hrabovský,[30] T. Huege,[37,15] A. Insolia,[54,44] P. G. Isar,[69] M. Ismaiel,[74,75] P. Janecek,[29] V. Jilek,[29] K.-H. Kampert,[34] B. Keilhauer,[37] A. Khakurdikar,[74] V. V. Kizakke Covilakam,[7,37] H. O. Klages,[37] M. Kleifges,[36] J. Köhler,[37] F. Krieger,[38] M. Kubatova,[29] N. Kunka,[36] B. L. Lago,[17] N. Langner,[38] N. Leal,[7] M. A. Leigui de Oliveira,[23] Y. Lema-Capeans,[73] A. Letessier-Selvon,[32] I. Lhenry-Yvon,[31] L. Lopes,[67] J. P. Lundquist,[70] M. Mallamaci,[57,44] S. Mancuso,[50,49] D. Mandat,[29] P. Mantsch,[§] A. G. Mariazzi,[3] C. Marinelli,[42,43] I. C. Mariş,[14] G. Marsella,[57,44] D. Martello,[52,45] S. Martinelli,[37,7] O. Martínez Bravo,[60] M. A. Martins,[73] H.-J. Mathes,[37] J. Matthews,[‖] G. Matthiae,[58,48] E. Mayotte,[78] S. Mayotte,[78] P. O. Mazur,[§] G. Medina-Tanco,[64] J. Meinert,[34] D. Melo,[7] A. Menshikov,[36] C. Merx,[37] S. Michal,[29] M. I. Micheletti,[5] L. Miramonti,[55,46] M. Mogarkar,[65] S. Mollerach,[1] F. Montanet,[*] L. Morejon,[34] K. Mulrey,[74,75] R. Mussa,[49] W. M. Namasaka,[34] S. Negi,[29] L. Nellen,[64] K. Nguyen,[80] G. Nicora,[9] M. Niechciol,[41] D. Nitz,[80] D. Nosek,[28] A. Novikov,[83] V. Novotny,[28] L. Nožka,[30] A. Nucita,[52,45] L. A. Núñez,[27] S. E. Nuza,[4] J. Ochoa,[7,37] M. Olegario,[19] C. Oliveira,[20] L. Östman,[29] M. Palatka,[29] J. Pallotta,[9] S. Panja,[29] G. Parente,[73] T. Paulsen,[34] J. Pawlowsky,[34] M. Pech,[29] J. Pękala,[65] R. Pelayo,[61] V. Pelgrims,[14] C. Pérez Bertolli,[7,37] L. Perrone,[52,45] S. Petrera,[42,43] C. Petrucci,[53] T. Pierog,[37] M. Pimenta,[67] M. Platino,[7] B. Pont,[74] M. Pourmohammad Shahvar,[57,44] P. Privitera,[82] C. Priyadarshi,[65] M. Prouza,[29] K. Pytel,[66] S. Querchfeld,[34] J. Rautenberg,[34] D. Ravignani,[7] J. V. Reginatto Akim,[21] A. Reuzki,[38] J. Ridky,[29] F. Riehn,[39,¶¶] M. Risse,[41] V. Rizi,[53,43] E. Rodriguez,[7,37] G. Rodriguez Fernandez,[48] J. Rodriguez Rojo,[11] S. Rossoni,[40] M. Roth,[37] E. Roulet,[1] A. C. Rovero,[4] A. Saftoiu,[68] M. Saharan,[74] F. Salamida,[53,43] H. Salazar,[60] G. Salina,[48] P. Sampathkumar,[37] N. San Martin,[78] J. D. Sanabria Gomez,[27] F. Sánchez,[7] F. M. Sánchez Rodriguez,[73] E. Santos,[29] F. Sarazin,[78] R. Sarmento,[67] R. Sato,[11] P. Savina,[42,43] V. Scherini,[52,45] H. Schieler,[37] M. Schimp,[34] D. Schmidt,[37] O. Scholten,[15,‖‖] H. Schoorlemmer,[74,75] P. Schovánek,[29] F. G. Schröder,[83,37] J. Schulte,[38] T. Schulz,[29] S. J. Sciutto,[3] M. Scornavacche,[7] A. Sedoski,[7] S. Sehgal,[34] S. U. Shivashankara,[70] G. Sigl,[40] K. Simkova,[15,14] F. Simon,[36] R. Šmída,[82] S. Soares Sippert,[25] P. Sommers,[¶] M. Stadelmaier,[37,46,55] S. Stanič,[70]

J. Stasielak,[65] P. Stassi,[*] S. Strähnz,[35] M. Straub,[38] T. Suomijärvi,[33] A. D. Supanitsky,[7] Z. Svozilikova,[29] Z. Szadkowski,[66] F. Tairli,[13] M. Tambone,[56,47] A. Tapia,[26] C. Taricco,[59,49] C. Timmermans,[75,74] O. Tkachenko,[29] P. Tobiska,[29] C. J. Todero Peixoto,[18] B. Tomé,[67] A. Travaini,[10] P. Travnicek,[29] C. Trimarelli,[42,43] M. Tueros,[3] M. Unger,[37] R. Uzeiroska-Geyik,[34] L. Vaclavek,[30] M. Vacula,[30] I. Vaiman,[42,43] J. F. Valdés Galicia,[64] L. Valore,[56,47] P. van Dillen,[74,75] E. Varela,[60] V. Vašíčková,[34] A. Vásquez-Ramírez,[27] D. Veberič,[37] I. D. Vergara Quispe,[3] S. Verpoest,[83] V. Verzi,[48] J. Vicha,[29] S. Vorobiov,[70] J. B. Vuta,[29] C. Watanabe,[25] A. A. Watson,[**] A. Weindl,[37] M. Weitz,[34] L. Wiencke,[78] H. Wilczyński,[65] B. Wundheiler,[7] B. Yue,[34] A. Yushkov,[29] E. Zas,[73] D. Zavrtanik,[70,71] and M. Zavrtanik[71,70]

(Pierre Auger Collaboration)[††,‡‡]

[1]Centro Atómico Bariloche and Instituto Balseiro (CNEA-UNCuyo-CONICET), San Carlos de Bariloche, Argentina
[2]Departamento de Física and Departamento de Ciencias de la Atmósfera y los Océanos, FCEyN, Universidad de Buenos Aires and CONICET, Buenos Aires, Argentina
[3]IFLP, Universidad Nacional de La Plata and CONICET, La Plata, Argentina
[4]Instituto de Astronomía y Física del Espacio (IAFE, CONICET-UBA), Buenos Aires, Argentina
[5]Instituto de Física de Rosario (IFIR)—CONICET/U.N.R. and Facultad de Ciencias Bioquímicas y Farmacéuticas U.N.R., Rosario, Argentina
[6]Instituto de Tecnologías en Detección y Astropartículas (CNEA, CONICET, UNSAM), and Universidad Tecnológica Nacional—Facultad Regional Mendoza (CONICET/CNEA), Mendoza, Argentina
[7]Instituto de Tecnologías en Detección y Astropartículas (CNEA, CONICET, UNSAM), Buenos Aires, Argentina
[8]International Center of Advanced Studies and Instituto de Ciencias Físicas, ECyT-UNSAM and CONICET, Campus Miguelete—San Martín, Buenos Aires, Argentina
[9]Laboratorio Atmósfera—Departamento de Investigaciones en Láseres y sus Aplicaciones—UNIDEF (CITEDEF-CONICET), Argentina
[10]Observatorio Pierre Auger, Malargüe, Argentina
[11]Observatorio Pierre Auger and Comisión Nacional de Energía Atómica, Malargüe, Argentina
[12]Universidad Tecnológica Nacional—Facultad Regional Buenos Aires, Buenos Aires, Argentina
[13]Adelaide University, Adelaide, South Australia, Australia
[14]Université Libre de Bruxelles (ULB), Brussels, Belgium
[15]Vrije Universiteit Brussels, Brussels, Belgium
[16]Centro Brasileiro de Pesquisas Fisicas, Rio de Janeiro, Rio de Janeiro, Brazil
[17]Centro Federal de Educação Tecnológica Celso Suckow da Fonseca, Petropolis, Brazil
[18]Universidade de São Paulo, Escola de Engenharia de Lorena, Lorena, São Paulo, Brazil
[19]Universidade de São Paulo, Instituto de Física de São Carlos, São Carlos, São Paulo, Brazil
[20]Universidade de São Paulo, Instituto de Física, São Paulo, São Paulo, Brazil
[21]Universidade Estadual de Campinas (UNICAMP), IFGW, Campinas, São Paulo, Brazil
[22]Universidade Estadual de Feira de Santana, Feira de Santana, Brazil
[23]Universidade Federal do ABC, Santo André, São Paulo, Brazil
[24]Universidade Federal do Paraná, Setor Palotina, Palotina, Brazil
[25]Universidade Federal do Rio de Janeiro, Instituto de Física, Rio de Janeiro, Rio de Janeiro, Brazil
[26]Universidad de Medellín, Medellín, Colombia
[27]Universidad Industrial de Santander, Bucaramanga, Colombia
[28]Charles University, Faculty of Mathematics and Physics, Institute of Particle and Nuclear Physics, Prague, Czech Republic
[29]Institute of Physics of the Czech Academy of Sciences, Prague, Czech Republic
[30]Palacky University, Olomouc, Czech Republic
[31]CNRS/IN2P3, IJCLab, Université Paris-Saclay, Orsay, France
[32]Laboratoire de Physique Nucléaire et de Hautes Energies (LPNHE), Sorbonne Université, Université de Paris, CNRS-IN2P3, Paris, France
[33]Université Paris-Saclay, CNRS/IN2P3, IJCLab, Orsay, France
[34]Bergische Universität Wuppertal, Department of Physics, Wuppertal, Germany
[35]Karlsruhe Institute of Technology (KIT), Institute for Experimental Particle Physics, Karlsruhe, Germany
[36]Karlsruhe Institute of Technology (KIT), Institut für Prozessdatenverarbeitung und Elektronik, Karlsruhe, Germany
[37]Karlsruhe Institute of Technology (KIT), Institute for Astroparticle Physics, Karlsruhe, Germany
[38]RWTH Aachen University, III. Physikalisches Institut A, Aachen, Germany
[39]TU Dortmund University, Department of Physics, Dortmund, Germany
[40]Universität Hamburg, II. Institut für Theoretische Physik, Hamburg, Germany
[41]Universität Siegen, Department Physik—Experimentelle Teilchenphysik, Siegen, Germany

[42]Gran Sasso Science Institute, L'Aquila, Italy
[43]INFN Laboratori Nazionali del Gran Sasso, Assergi (L'Aquila), Italy
[44]INFN, Sezione di Catania, Catania, Italy
[45]INFN, Sezione di Lecce, Lecce, Italy
[46]INFN, Sezione di Milano, Milano, Italy
[47]INFN, Sezione di Napoli, Napoli, Italy
[48]INFN, Sezione di Roma "Tor Vergata," Roma, Italy
[49]INFN, Sezione di Torino, Torino, Italy
[50]Osservatorio Astrofisico di Torino (INAF), Torino, Italy
[51]Politecnico di Milano, Dipartimento di Scienze e Tecnologie Aerospaziali, Milano, Italy
[52]Università del Salento, Dipartimento di Matematica e Fisica "E. De Giorgi," Lecce, Italy
[53]Università dell'Aquila, Dipartimento di Scienze Fisiche e Chimiche, L'Aquila, Italy
[54]Università di Catania, Dipartimento di Fisica e Astronomia "Ettore Majorana," Catania, Italy
[55]Università di Milano, Dipartimento di Fisica, Milano, Italy
[56]Università di Napoli "Federico II," Dipartimento di Fisica "Ettore Pancini," Napoli, Italy
[57]Università di Palermo, Dipartimento di Fisica e Chimica "E. Segrè," Palermo, Italy
[58]Università di Roma "Tor Vergata," Dipartimento di Fisica, Roma, Italy
[59]Università Torino, Dipartimento di Fisica, Torino, Italy
[60]Benemérita Universidad Autónoma de Puebla, Puebla, México
[61]Unidad Profesional Interdisciplinaria en Ingeniería y Tecnologías Avanzadas del Instituto Politécnico Nacional (UPIITA-IPN), México, Distrito Federal, México
[62]Universidad Autónoma de Chiapas, Tuxtla Gutiérrez, Chiapas, México
[63]Universidad Michoacana de San Nicolás de Hidalgo, Morelia, Michoacán, México
[64]Universidad Nacional Autónoma de México, México, Distrito Federal, México
[65]Institute of Nuclear Physics PAN, Krakow, Poland
[66]University of Łódź, Faculty of High-Energy Astrophysics,Łódź, Poland
[67]Laboratório de Instrumentação e Física Experimental de Partículas—LIP and Instituto Superior Técnico—IST, Universidade de Lisboa—UL, Lisboa, Portugal
[68]"Horia Hulubei" National Institute for Physics and Nuclear Engineering, Bucharest-Magurele, Romania
[69]Institute of Space Science, Bucharest-Magurele, Romania
[70]Center for Astrophysics and Cosmology (CAC), University of Nova Gorica, Nova Gorica, Slovenia
[71]Experimental Particle Physics Department, J. Stefan Institute, Ljubljana, Slovenia
[72]Universidad de Granada and C.A.F.P.E., Granada, Spain
[73]Instituto Galego de Física de Altas Enerxías (IGFAE), Universidade de Santiago de Compostela, Santiago de Compostela, Spain
[74]IMAPP, Radboud University Nijmegen, Nijmegen, The Netherlands
[75]Nationaal Instituut voor Kernfysica en Hoge Energie Fysica (NIKHEF), Science Park, Amsterdam, The Netherlands
[76]Stichting Astronomisch Onderzoek in Nederland (ASTRON), Dwingeloo, The Netherlands
[77]Case Western Reserve University, Cleveland, Ohio, USA
[78]Colorado School of Mines, Golden, Colorado, USA
[79]Department of Physics and Astronomy, Lehman College, City University of New York, Bronx, New York, USA
[80]Michigan Technological University, Houghton, Michigan, USA
[81]New York University, New York, New York, USA
[82]University of Chicago, Enrico Fermi Institute, Chicago, Illinois, USA
[83]University of Delaware, Department of Physics and Astronomy, Bartol Research Institute, Newark, Delaware, USA
[84]Institut universitaire de France (IUF), France

(Received 18 February 2026; revised 22 April 2026; accepted 22 May 2026; published 8 September 2026)

[*]Université Grenoble Alpes, CNRS, Grenoble Institute of Engineering, LPSC-IN2P3, Grenoble, France.
[†]Max-Planck-Institut für Radioastronomie, Bonn, Germany.
[‡]Colorado State University, Fort Collins, Colorado, USA.
[§]Fermi National Accelerator Laboratory, Fermilab, Batavia, Illinois, USA.
[‖]Louisiana State University, Baton Rouge, Louisiana, USA.
[¶]Pennsylvania State University, University Park, Pennsylvania, USA.
[**]School of Physics and Astronomy, University of Leeds, Leeds, United Kingdom.
[††]Pierre Auger spokesperson: spokespersons@auger.org
[‡‡]http://www.auger.org
[§§]Present address: Graduate School of Science, Osaka Metropolitan University, Osaka, Japan.
[‖‖]Also at Kapteyn Institute, University of Groningen, Groningen, The Netherlands.
[¶¶]Present address: Technische Universität Dortmund and Ruhr-Universität Bochum, Dortmund and Bochum, Germany.

Quantum gravity theories often modify spacetime symmetries. In particular, Lorentz invariance may be violated when approaching the Planck scale. Although the scales at which interactions occur in extensive air showers induced by ultra-high-energy cosmic rays in the atmosphere are many orders of magnitude below the Planck scale, these violations might still be observable. In this Letter, the fluctuations in the number of muons in the extensive air showers measured at the Pierre Auger Observatory are exploited, for the first time, to constrain Lorentz invariance violations. The bounds derived in the hadronic sector are the strongest ever obtained, and do not rely on assumptions about the mass composition of ultra-high-energy cosmic rays. The fluctuations in the number of muons constitute a new and powerful observable to further explore Lorentz invariance in a region of the parameter space not accessible to other observables.

DOI: 10.1103/t5k4-2m32

The effort for a unified theory of gravity has led to the development of several quantum gravity (QG) models, some of them implying the breaking of Lorentz invariance (LI) [1]. While this would appear at the scale of the Planck mass, the highest energetic processes in our Universe, namely, those involving the interactions of ultra-high-energy cosmic rays (UHECRs), could keep track of this breaking. During their propagation in extragalactic space, UHECRs undergo interactions with background photons such as meson photoproduction or photodisintegration; Lorentz invariance violations (LIV) could affect their energy thresholds, suppressing such interactions and making the attenuation lengths extremely large [1–4]. As a consequence, the existing evidence of the suppression of the UHECR flux at the highest energies [5,6] can be exploited to set limits on LIV. In particular, LIV can be tested by searching for the best description of UHECR observables in terms of astrophysical scenarios, under LIV assumptions, as already attempted, for instance, in [7–12]. However, the scenario is complicated by the fact that the best astrophysical description of the UHECR energy spectrum and mass composition is found corresponding to values of maximum energy of UHECRs at the sources smaller than or comparable to the typical threshold energy for photomeson or photodisintegration reactions [13,14]. For this reason, the sensitivity to deviations from LI in the UHECR propagation is milder than expected, and alternative approaches need to be investigated. Independently of propagation effects, Lorentz invariance violation may also manifest itself in particle interactions at extreme energies, potentially altering the development of extensive air showers in the atmosphere. Depending on the strength of the LI violation, the high energies available in the collision of cosmic rays with the atmosphere [15] can lead to modifications of the shower development with respect to the standard LI case [9], which is what is investigated in this Letter. The Pierre Auger Observatory [16], located near Malargüe, in the Province of Mendoza in Argentina, is the largest cosmic-ray detector ever constructed, covering an area of 3000 km^2. Completed in 2008, it serves as the most precise facility for UHECR detection above 0.1 EeV. The basic design of the observatory comprises two components: the surface detector (SD) array, featuring 1660 water Cherenkov detectors (WCD) arranged in a triangular grid, and the fluorescence detector (FD), a set of telescopes overlooking the SD area. The SD, designed for nearly 100% duty cycle operation, detects secondary particles at the ground level, while the FD, operational on clear moonless nights with a ∼15% duty cycle, captures UV fluorescence light emitted by nitrogen molecules along the path of extensive air showers (EAS). This hybrid configuration guarantees a thorough comprehension of UHECRs by combining a detailed calorimetric measurement of the longitudinal profile with the FD, and assessing the lateral distribution of particles at ground through the SD. In 2015, the Pierre Auger Collaboration initiated a crucial upgrade phase known as AugerPrime [17]. The upgrade significantly improves the observatory's ability to discriminate muonic and electromagnetic components of showers on an event-by-event basis, offering valuable insights into UHECR physics. The Pierre Auger Observatory can measure the fluctuations in the number of muons using a subset of inclined hybrid events ($62° < \theta < 80°$) reconstructed simultaneously by the SD and FD, for which the pure electromagnetic component is largely absorbed in the atmosphere and the particles reaching the ground directly sample the muon content. The measurement used in this Letter is based on data collected between January 1, 2004 and December 31, 2017; after the full event selection, 786 events remain, of which 281 with energy $E > 4 \times 10^{18}$ eV are used to extract the fluctuations, thus ensuring the full trigger efficiency for the SD. Within the current uncertainties, an agreement between the experimental relative fluctuations and the models has been found [18]. In this context, the event-by-event fluctuations in the number of muons at ground provide a particularly sensitive probe, as they are dominated by the first hadronic interactions and are less affected by the overall normalization and mass composition uncertainties. In this Letter, for the first time, measurements of the relative fluctuations in the number of muons [19] in extensive air showers are exploited to constrain LIV in the hadronic sector, in a region of parameter space not accessible to the LIV modifications in the extragalactic propagation of cosmic rays.

Lorentz invariance violation framework—A well-established phenomenological approach to introduce LIV effects consists of adding effective terms in the dispersion relation of a particle, arising from a metric modification (see Ref. [1] for details). The dispersion relation would therefore appear as

$$E^2 - p^2 = m^2 + f(\vec{p}, M_{\rm Pl}), \tag{1}$$

where m is the particle mass, E its energy, $\vec{p}$ its momentum, and $M_{\rm Pl}$ is the Planck mass [20]. At $|\vec{p}| \ll M_{\rm Pl}$, f can be expanded in series and considering only the leading order of the expansion, n, Eq. (1) becomes

$$E^2 - p^2 = m^2 + \eta^{(n)} \frac{p^{n+2}}{M_{\rm Pl}^n}, \tag{2}$$

where η is the dimensionless constant coefficient to be constrained.

The LIV hadronic sector is investigated through the expected cosmic-ray flux at Earth, compared to the measured energy spectrum and mass composition. Negative values of η do not imply significant changes in the propagation of UHECRs [9,10]; in [12], positive values of η are explored setting upper limits for different orders of violation, achieved through the flux suppression observed at the highest energies: $\eta_\pi^{(1)} < 2.4 \times 10^{-10}$ and $\eta_\pi^{(2)} < 0.3$, at 5σ CL [21]. The second order LIV parameter in the hadronic sector is also investigated in previous works, such as [3] with similar conclusions as in [12] although with assumptions on the UHECR mass composition [22]. Interpreting the right-hand side of the Eq. (2) as an energy dependent mass:

$$m_{\rm LIV}^2 = m^2 + \eta^{(n)} \frac{p^{n+2}}{M_{\rm Pl}^n}, \tag{3}$$

the Lorentz factor for a LI violating particle at energy E can be defined as

$$\gamma_{\rm LIV} = E/m_{\rm LIV}. \tag{4}$$

Depending on the value assumed by $\eta^{(n)}$, the lifetime of the considered particle $\tau = \gamma_{\rm LIV}\tau_0$ will change accordingly. For negative or positive values of $\eta^{(n)}$, the lifetime of the particle should increase or decrease with respect to the LI case producing modifications in the EAS development. As an example, the π^0 lifetime as a function of the energy for the standard case and for different values of the LIV parameter is shown in Fig. 1.

For negative values of η, the mean lifetime increases up to a critical energy, corresponding to the point at which the phase space reduces to zero (i.e., $m_{\rm LIV}^2 \to 0$) and the particle becomes stable (i.e., $\gamma \to \infty$). The energy at which the lifetime evolution deviates from the LI case depends both on the order and the strength of the violation. On the other hand, for positive values of the eta parameter the lifetime becomes smaller with respect to the standard LI case as the energy increases. Since neutral pions already decay promptly in the Lorentz-invariant case, the corresponding effects are expected to be much smaller for the observable considered here. For this reason, in this Letter we only focus on negative values of the η parameter. In order to describe the modifications in the development of a shower, let us first consider the simple model [24], where a primary hadron interacts in the atmosphere, transferring a fraction $\alpha_{\rm had,1}$ of its energy to hadronic particles (mainly charged pions, $\pi^\pm$), while the remaining $(1-\alpha_{\rm had,1})$ fraction goes to neutral pions, π^0. Charged pions further interact, developing a hadronic cascade, while neutral pions decay promptly into photons, forming an electromagnetic subshower. The number of charged pions grows with each generation i until energy depletion. At the critical generation $i = c$, charged pions predominantly decay into muons, yielding

$$N_\mu = \frac{E_0}{\xi_c} \prod_{i=1}^{c} \alpha_{{\rm had},i}, \tag{5}$$

where E_0 is the primary energy and ξ_c the pion critical energy. Fluctuations in N_μ arise from variations in $\alpha_{{\rm had},i}$:

$$\left(\frac{\sigma_{N_\mu}}{\langle N_\mu \rangle}\right)^2 = \sum_{i=1}^{c} \left(\frac{\sigma(\alpha_{{\rm had},i})}{\langle \alpha_{{\rm had},i} \rangle}\right)^2. \tag{6}$$

For large i, $\sigma(\alpha_{{\rm had},i})$ decreases as $\alpha_{{\rm had},i}$ averages over many interactions, making $\sigma(\alpha_{\rm had,1})$ dominant [25]. In the LIV scenario with negative $\eta^{(n)}$, the π^0 lifetime increases, enhancing interaction probability before decay. This

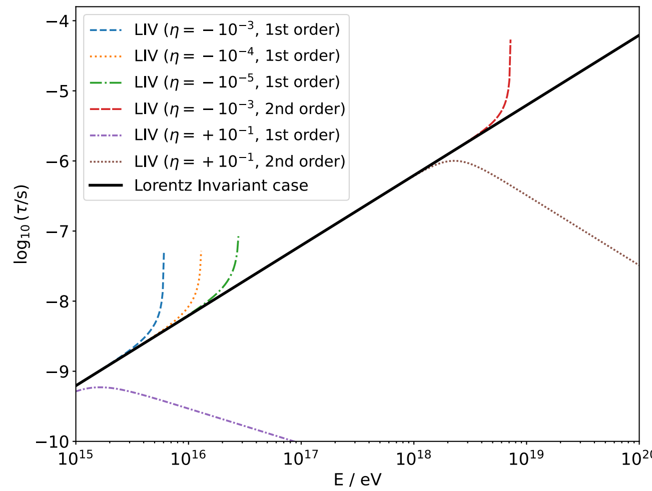

FIG. 1. Mean lifetime of the neutral pion as a function of the energy for the Lorentz invariant case and for different strengths and orders of LIV.

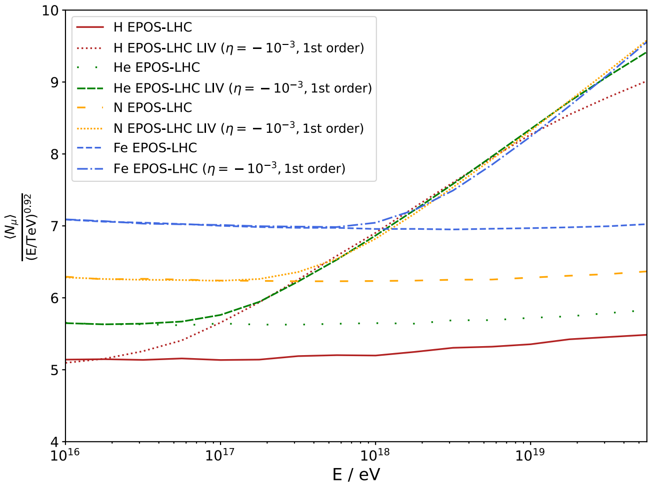

FIG. 2. Average number of muons at ground vs primary energy in LI and LIV cases.

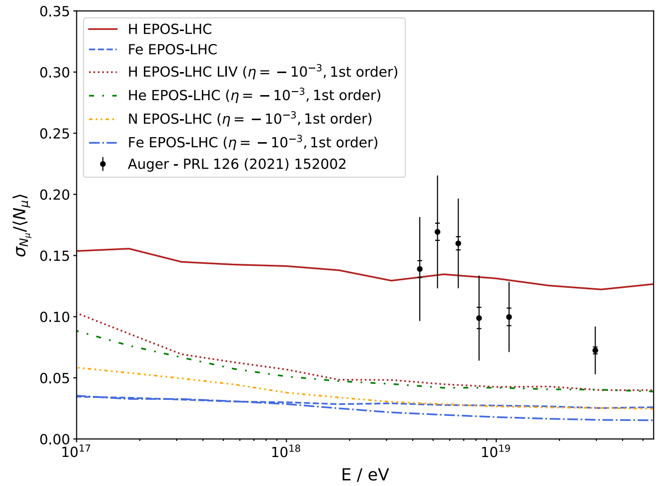

FIG. 3. Relative fluctuation of the number of muons vs primary energy; data (black points, from [18]; the statistical uncertainty is indicated by the error bars, while the total systematic uncertainty by the square brackets) are compared to expectations from LI and LIV ($\eta = -10^{-3}$) models.

causes neutral pions to initiate hadronic sub-showers. As $\alpha_{\mathrm{had},j}^{\mathrm{LIV}} \simeq 1$ for affected generations, fluctuations diminish $[\sigma(\alpha_{\mathrm{had},j}^{\mathrm{LIV}}) \simeq 0]$ and only LI generations contribute to fluctuations in Eq. (8). The number of muons, on the other hand, increases by $\prod_{j=1}(\alpha_{\mathrm{had},j}^{\mathrm{LIV}} - \alpha_{\mathrm{had},j})$. In summary, LIV leads to a moderate muon excess and reduced fluctuations due to limited stochastic leakage in the first interaction [25].

Since less energy is transferred to the electromagnetic component, the shower maximum depth ($X_{\max}$ [26]) is slightly modified, and a displacement in the position of the maximum of the longitudinal profile is expected, together with a reduction of the maximum energy deposit in the atmosphere (see Supplemental Material [28]).

Simulating LIV effects in the shower development—To quantify the effect of LIV on the shower development, we have performed detailed simulations of its longitudinal profile by using the CONEX software [29,30] for the LI and LIV cases. For the LIV scenario, the software has been modified by changing the lifetime of any unstable particle according to Eq. (4). The $\eta^{(n)}$ values considered in this Letter span the range from -10^{-1} to -10^{-6} in logarithmic steps, with order of violation $n = 1$. For each value of η, 15 000 primary cosmic-ray particles have been produced in the energy range between 10^{14} and 10^{21} eV, using EPOS-LHC [31] and QGSJetII-04 [32] hadronic interaction models and for different primary particle types, i.e., hydrogen, helium, nitrogen, and iron nuclei.

The enhanced number of interactions of neutral pions due to LIV contributes to the growth of the hadronic component in the cascade producing an increase in the number of muons N_μ, as shown in Fig. 2, where the average number of muons at ground as a function of the primary energy in LI and LIV cases are shown. In the LIV scenarios considered here, the number of muons increases for any primary mass once the energy threshold is surpassed, where pions in the shower become stable. For iron primaries, this threshold occurs at higher energies due to their larger mass, as can be understood through a simple superposition model for nuclei with $A > 1$. Once LIV is in place, the rate of muon increase is similar for protons, iron, and intermediate masses. However, at the highest energies, the number of muons for heavier nuclei exceeds that of protons, as protons saturate earlier, when all available pions in the showers are interacting instead of decaying. This fact affects the fluctuations of the number of muons. In fact, the ratio of the fluctuations to the average number of muons (hereinafter referred to as relative fluctuations), dominated mostly by the first interaction [25], considerably decreases in the presence of LIV for the case of protons, as shown in Fig. 3. The decrease is due at the same time to the increase of the N_μ and to the decrease of fluctuations induced by LIV effects. The decrease is milder for heavier nuclear species.

Limits on the LIV parameter η can be derived by comparing the expected decrease of the relative fluctuations caused by LIV effects with the experimental measurements [18].

Results and discussion—The relative fluctuations in the number of muons are directly linked to the mass composition of UHECRs, which consist of a mixture of nuclear species arriving at Earth [33,34]. An accurate determination of the contribution of different nuclear species to the UHECR flux is challenging due to uncertainties in the hadronic interaction models used to describe the shower development at these extreme energies. These models, which describe key processes such as particle production and energy dissipation, significantly influence the inferred composition. Thus, any attempt to constrain the degree of LIV in EAS development must account for these uncertainties.

To this aim, we notice that in the case of a composition comprised of the lightest and heaviest nuclear species (p and Fe, respectively), the width of the distribution of the shower maxima is the largest, as shown, for instance, in [35]. The same behavior can be expected for the relative muon fluctuations. Although when LIV is included the relative fluctuations in the number of muons differ only slightly among different primaries (as shown in the highest energy range in Fig. 3), they are maximized when considering a mixed composition of protons and iron nuclei. The robustness of this choice against alternative mixtures, including intermediate masses, is illustrated in the Supplemental Material [28] through the corresponding so-called umbrella plots which illustrate the allowed phase space of fluctuations average and average of the number of muons. These show that, in the region relevant to this analysis, the hierarchy of relative muon fluctuations is largely preserved and intermediate-mass combinations do not exceed the proton-iron benchmark. This makes the proton-iron mixture a conservative benchmark for the present exclusion procedure.

As described in [18], the average number of muons, $\langle N_\mu \rangle_{\rm mix}$, and its fluctuations, $\sigma_{N_\mu,{\rm mix}}$, can be calculated for a mixture of p and Fe as follows:

$$\begin{aligned} \langle N_\mu \rangle_{\rm mix}(f;\eta) &= (1-f)\langle N_\mu \rangle_{\rm p} + f\langle N_\mu \rangle_{\rm Fe} \\ \sigma^2_{N_\mu,{\rm mix}}(f;\eta) &= (1-f)\sigma^2_{N_\mu,{\rm p}} + f\sigma^2_{N_\mu,{\rm Fe}} \\ &\quad + f(1-f)(\langle N_\mu \rangle_{\rm p} - \langle N_\mu \rangle_{\rm Fe})^2 \end{aligned} \tag{7}$$

where f, which depends on the energy, is the relative abundance of iron nuclei [36]. The average number of muons $\langle N_\mu \rangle$ and the $\sigma^2_{N_\mu}$ for air showers induced by both proton and iron nuclei have been obtained from the air shower simulations performed with different LIV parameters over the energy range reported in the previous section. These results have been used to parametrize $\langle N_\mu \rangle$ and σ_{N_μ} across the range $E = 10^{14}$ eV to $E = 10^{20}$ eV, for $-10^{-1} < \eta < -10^{-6}$ and for both proton and iron primaries. These parametrizations were then extrapolated to provide expectations in the energy range 10^{16} to 10^{20} eV and for η values extended down to -10^{-16} (see Supplemental Material [28]). For any given value of η, the parametrizations allow us to calculate the expected relative fluctuations for a specific mixture of proton and iron nuclei (hereinafter referred to as mixed relative fluctuations) as follows:

$$\frac{\sigma_{N_\mu}}{\langle N_\mu \rangle}(f;\eta) = \frac{\sqrt{\sigma^2_{N_\mu,{\rm mix}}(N_\mu)(f;\eta)}}{\langle N_\mu \rangle_{\rm mix}(f;\eta)}. \tag{8}$$

To identify the most conservative LIV model, the relative fluctuations are analyzed as a function of energy by determining the value of f that maximizes the mixed fluctuations for each energy bin. This maximum, determined by varying f between 0 and 1 (i.e., scanning from a pure proton to a pure iron composition), is found to be consistent across all tested values of the LIV parameter η (see Supplemental Material [28]). Consequently, the most conservative LIV model for any composition corresponds to the values $f(E)$ that maximize Eq. (8), under the constraint that the predicted curves lie entirely below the measured data. Notably, this procedure allows the most conservative LIV relative fluctuations to be determined for any given LIV parameter value without requiring additional shower simulations.

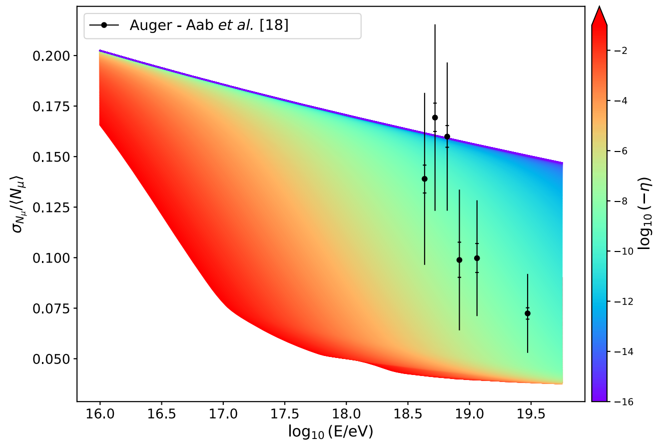

FIG. 4. Mixed relative fluctuations obtained using the parameterisations considering η in the range $[-10^{-1}, -10^{-16}]$ as a function of the primary energy, corresponding to the maximum with respect to f. Each color corresponds to a different violation strength (right axis, where the arrow indicates the direction of increasing violation strength). The measured relative fluctuations in the number of muons are shown with black points [18].

In Fig. 4, the color code represents the relative fluctuations corresponding to the maxima with respect to f, derived from the parametrizations considering η values in the range $[-10^{-1}, -10^{-16}]$. By selecting only the mixed relative fluctuations below the experimental data points, the χ^2 is computed as a function of η. This approach yields a continuous confidence level for excluding specific LIV models, allowing the determination of the strictest lower bound on η.

The mixed relative fluctuations have been estimated for three different confidence levels (CLs) by considering all available experimental data. The exclusion limits for η, quantified as $\log_{10}(-\eta)$, represent the smallest level of violation that can be ruled out at each corresponding

TABLE I. Lower limits on $\log_{10}(-\eta)$ derived from this analysis at different confidence levels. The asymmetric uncertainties indicate the associated systematic uncertainty from the spread between the EPOS-LHC and QGSJetII-04 predictions.

CL	90.5%	95.5%	99.9%
$\log_{10}(-\eta)$	$-7.03^{+0.21}_{-0.50}$	$-6.82^{+0.19}_{-0.54}$	$-5.90^{+0.13}_{-0.62}$

confidence level. The exclusion limits at the 99.9%, 95.5%, and 90.5% CLs are summarized in Table I. These bounds were determined independently using two distinct hadronic interaction models, EPOS-LHC and QGSJetII-04. The quoted central value is the mean of the two results, while the spread between them is taken as an estimate of the systematic uncertainty associated with the hadronic interaction modeling.

It can be observed that, if the discrepancy in the energy reconstruction between the LIV scenario and the standard one were explicitly accounted for, a shift in the experimental data towards higher reconstructed energies would occur. This is because, in the LIV scenario, a smaller fraction of the primary energy is transferred to the electromagnetic component of the shower, which is used to reconstruct the energy. However, this bias in the energy estimation between the two scenarios remains below 5% for all the considered η parameter values. As a result, incorporating this effect into the analysis would change the reconstructed energy values leading to a more stringent constraint on the η parameter.

Conclusions—In this Letter, interactions of particles at the most extreme energies have been exploited to test Lorentz invariance, a frontier in physics which is reminiscent of the early 20th century, when cosmic rays paved the future of particle physics. A significant milestone in constraining first-order Lorentz invariance violation has been achieved through the analysis of muon fluctuations within extensive air showers—used for the first time to this purpose—measured at the Pierre Auger Observatory. Using a conservative model based on mixed nuclear composition of protons and iron nuclei, we derived the most stringent LIV bounds, for negative values of the LIV parameter: $\eta_\pi > -1.26 \times 10^{-6}$ at 5σ CL. Upper bounds are instead obtained with studies considering UHECR propagation, which find that $\eta_\pi < 2.4 \times 10^{-10}$ at 5σ CL. In addition to showing the potential of muon-related observables to detect deviations from Lorentz invariance, with this Letter we demonstrate the unique capability of testing both negative and positive values of LIV parameters exploiting at most the data of the same observatory. Future efforts will be devoted to extend this analysis to investigating second-order LIV effects and combining muon fluctuation data with mass composition estimates and other observables, such as radio detector data [37] and underground muon detector (UMD) measurements [37].

In summary, this Letter represents a foundational step towards a comprehensive test of Lorentz invariance at ultrahigh energies, as aimed in [38], thanks to the unique capability of the Pierre Auger Observatory to explore extreme energy scales.

Acknowledgments—The successful installation, commissioning, and operation of the Pierre Auger Observatory would not have been possible without the strong commitment and effort from the technical and administrative staff in Malargüe. We are very grateful to the following agencies and organizations for financial support: Argentina—Comisión Nacional de Energía Atómica; Agencia Nacional de Promoción Científica y Tecnológica (ANPCyT); Consejo Nacional de Investigaciones Científicas y Técnicas (CONICET); Gobierno de la Provincia de Mendoza; Municipalidad de Malargüe; NDM Holdings and Valle Las Leñas; in gratitude for their continuing cooperation over land access; Australia—the Australian Research Council; Belgium—Fonds de la Recherche Scientifique (FNRS); Research Foundation Flanders (FWO), Marie Curie Action of the European Union Grant No. 101107047; Brazil—Ministério da Ciência, Tecnologia e Inovação (MCTI); Czech Republic—GACR 24-13049S, CAS LQ100102401, MEYS LM2023032, CZ.02.1.01/0.0/0.0/16_013/0001402, CZ.02.1.01/0.0/0.0/18_046/0016010, CZ.02.1.01/0.0/0.0/17_049/0008422, and CZ.02.01.01/00/22_008/0004632; France—Centre de Calcul IN2P3/CNRS; Centre National de la Recherche Scientifique (CNRS); Institut National de Physique Nucléaire et de Physique des Particules (IN2P3/CNRS); Germany—Bundesministerium für Forschung, Technologie und Raumfahrt (BMFTR); Deutsche Forschungsgemeinschaft (DFG); Ministerium für Finanzen Baden-Württemberg; Helmholtz Alliance for Astroparticle Physics (HAP); Hermann von Helmholtz-Gemeinschaft Deutscher Forschungszentren e.V.; Ministerium für Kultur und Wissenschaft des Landes Nordrhein-Westfalen; Ministerium für Wissenschaft, Forschung und Kunst des Landes Baden-Württemberg; Italy—Istituto Nazionale di Fisica Nucleare (INFN); Istituto Nazionale di Astrofisica (INAF); Ministero dell'Università e della Ricerca (MUR); CETEMPS Center of Excellence; Ministero degli Affari Esteri (MAE), ICSC Centro Nazionale di Ricerca in High Performance Computing, Big Data and Quantum Computing, funded by European Union NextGenerationEU, reference code CN_00000013; México—Consejo Nacional de Ciencia y Tecnología (CONACYT-SECHTI) No. CB-A1-S-46703, Universidad Nacional Autónoma de México (UNAM) PAPIIT-IN114924; Benemérita Universidad Autónoma de Puebla (BUAP), VIEP and Laboratorio Nacional de Supercómputo del Sureste de México (LNS); and Benemérita Universidad Autónoma de Chiapas (UNACH); The Netherlands—Ministry of Education, Culture and Science; Netherlands Organisation for Scientific Research (NWO); Dutch national e-infrastructure with the support of SURF Cooperative; Poland—Ministry of Science and Higher Education, Grant No. 2022/WK/12; National Science Centre, Grants No. 2020/39/B/ST9/01398, and No. 2022/45/B/ST9/02163; Portugal—Portuguese national funds and FEDER funds within Programa Operacional Factores de Competitividade through Fundação para a

Ciência e a Tecnologia (COMPETE); Romania—Ministry of Education and Research, Contract No. 30N/2023 under Romanian National Core Program LAPLAS VII, and Grant No. PN 23 21 01 02; Slovenia—Slovenian Research and Innovation Agency, Grants No. P1-0031 and No. I0-0033; Spain—Ministerio de Ciencia, Innovación y Universidades/Agencia Estatal de Investigación MICIU/AEI /10.13039/501100011033 (PID2022-140510NB-I00, PCI2023-145952-2, CNS2024-154676, and María de Maeztu CEX2023-001318-M), Xunta de Galicia (CIGUS Network of Research Centers, Consolidación ED431C-2025/11 and ED431F-2022/15) and European Union ERDF; USA—Department of Energy, Contracts No. DE-AC02-07CH11359, No. DE-FR02-04ER41300, No. DE-FG02-99ER41107, and No. DE-SC0011689; National Science Foundation, Grants No. 0450696, and No. NSF-2013199; The Grainger Foundation; Astrophysics Centre for Multi-messenger studies in Europe (ACME) EU Grant No. 101131928; and UNESCO.

Data availability—The data that support the findings of this article are not publicly available. The data are available from the authors upon reasonable request.

[1] R. Aloisio, P. Blasi, P. L. Ghia, and A. F. Grillo, Phys. Rev. D **62**, 053010 (2000).

[2] F. W. Stecker and S. T. Scully, New J. Phys. **11**, 085003 (2009).

[3] L. Maccione, A. M. Taylor, D. M. Mattingly, and S. Liberati, J. Cosmol. Astropart. Phys. 04 (2009) 022.

[4] A. Saveliev, L. Maccione, and G. Sigl, J. Cosmol. Astropart. Phys. 03 (2011) 046.

[5] A. Aab *et al.* (Pierre Auger Collaboration), Phys. Rev. D **102**, 062005 (2020).

[6] A. Abdul Halim *et al.* (Pierre Auger Collaboration), Phys. Rev. Lett. **135**, 241002 (2025).

[7] X.-J. Bi, Z. Cao, Y. Li, and Q. Yuan, Phys. Rev. D **79**, 083015 (2009).

[8] S. T. Scully and F. W. Stecker, Astropart. Phys. **31**, 220 (2009).

[9] D. Boncioli, A. di Matteo, F. Salamida, R. Aloisio, P. Blasi, P. L. Ghia, A. Grillo, S. Petrera, and T. Pierog, Proc. Sci. ICRC2015 (**2016**) 521 [arXiv:1509.01046].

[10] D. Boncioli (Pierre Auger Collaboration), Proc. Sci ICRC2017 (**2018**) 561.

[11] R. G. Lang (Pierre Auger Collaboration), Proc. Sci. ICRC2019 (**2020**) 327.

[12] P. Abreu *et al.* (Pierre Auger Collaboration), J. Cosmol. Astropart. Phys. 01 (2022) 023.

[13] A. Aab *et al.* (Pierre Auger Collaboration), J. Cosmol. Astropart. Phys. 04 (2017) 038; 03 (2018) E02.

[14] A. A. Halim *et al.* (Pierre Auger Collaboration), J. Cosmol. Astropart. Phys. 05 (2023) 024.

[15] A proton at 10^{19} eV hitting the atmosphere corresponds to a 0.1 PeV collision in the center-of-mass frame.

[16] A. Aab *et al.* (Pierre Auger Collaboration), Nucl. Instrum. Methods Phys. Res., Sect. A **798**, 172 (2015).

[17] D. Schmidt (Pierre Auger Collaboration), Proc. Sci. ICRC2025 (**2025**) 385 [arXiv:2508.08056].

[18] A. Aab *et al.* (Pierre Auger Collaboration), Phys. Rev. Lett. **126**, 152002 (2021).

[19] P. Abreu *et al.* (Pierre Auger Collaboration), Proc. Sci. ICRC2021 (**2021**) 340.

[20] Natural units are used hereinafter.

[21] The reported values are for η_π, which can be computed from η_p (the LIV parameter for the proton) as $\eta_\pi \approx 2\eta_\mathrm{p}$ in the approximation given in [8]. The relation between η_p and the corresponding parameter for other nuclei can be derived by the superposition model as done in [12].

[22] For a collection of results on LIV studies, see Ref. [23].

[23] A. Addazi *et al.*, Prog. Part. Nucl. Phys. **125**, 103948 (2022).

[24] J. Matthews, Astropart. Phys. **22**, 387 (2005).

[25] L. Cazon, R. Conceição, and F. Riehn, Phys. Lett. B **784**, 68 (2018).

[26] X_max is defined as the depth in the atmosphere at which the EAS reaches its maximum number of particles. It is sensitive to the mass composition of the primary cosmic ray [27].

[27] J. Linsley and A. A. Watson, Phys. Rev. Lett. **46**, 459 (1981).

[28] See Supplemental Material at http://link.aps.org/supplemental/10.1103/t5k4-2m32 for the umbrella plots.

[29] T. Pierog *et al.*, Nucl. Phys. B, Proc. Suppl. **151**, 159 (2006).

[30] T. Bergmann, R. Engel, D. Heck, N. N. Kalmykov, S. Ostapchenko, T. Pierog, T. Thouw, and K. Werner, Astropart. Phys. **26**, 420 (2007).

[31] T. Pierog, I. Karpenko, J. M. Katzy, E. Yatsenko, and K. Werner, Phys. Rev. C **92**, 034906 (2015).

[32] S. Ostapchenko, Phys. Rev. D **83**, 014018 (2011).

[33] A. Aab *et al.* (Pierre Auger Collaboration), Phys. Rev. D **90**, 122005 (2014).

[34] A. Aab *et al.* (Pierre Auger Collaboration), Phys. Rev. D **90**, 122006 (2014).

[35] K.-H. Kampert and M. Unger, Astropart. Phys. **35**, 660 (2012).

[36] $\langle N_\mu \rangle_\mathrm{p}$, $\langle N_\mu \rangle_\mathrm{Fe}$, $\sigma^2_{N_\mu,\mathrm{p}}$ and $\sigma^2_{N_\mu,\mathrm{Fe}}$ depend on energy and on the LIV parameter η.

[37] F. Salamida (Pierre Auger Collaboration), Proc. Sci. ICRC2023 (**2023**) 016 [arXiv:2312.14673].

[38] R. Alves Batista *et al.*, Classical Quantum Gravity **42**, 032001 (2025).